A Passive Magnet Bearing System for Energy Storage Flywheels

H. Ming Chen, Thomas Walter, Scott Wheeler, Nga Lee
Foster-Miller Technologies
431 New Karner Road, Albany, NY 12205-3868, USA
mchen@fosmiltech.com

ABSTRACT

For flywheel applications, a passive magnet bearing system including two radial permanent-magnet bearings, an active thrust bearing, and an active radial damper has been tested to 50,000 rpm. Test results have verified the need for and predicted performance of the active radial damper for the passive bearing system.

INTRODUCTION

Passive magnetic bearings made of permanent magnets (PMs) are common [1, 2] but seldom used for high-speed applications, such as energy storage flywheels. The advantages of passive bearings include structural simplicity and insignificant energy loss, since they do not require control electronics or a power source. However, for a passive bearing to provide practical stiffness, PMs on both stator and rotor are required, but retention of the rotor magnets at high rotating speed is not a trivial design and fabrication challenge. Another concern for the rotor dynamics is the lack of damping in the passive bearing. In the typical speed range of an energy storage flywheel (30,000 to 60,000 rpm), the shaft typically traverses two or more critical speeds and many structural resonance frequencies. Without proper system damping, the rotor risks vibration from synchronous and harmonic excitation due to unbalance, as well as catastrophic subsynchronous whirls.

With these considerations in mind, a passive magnet bearing system has been developed for flywheels used in space energy storage systems or terrestrial applications. The system includes: two radial passive magnet bearings, an active radial damper, an active thrust bearing, and ride-through auxiliary bearings to center and clamp the shaft during launch and on-orbit maneuvers. As related herein, we have designed and fabricated the system and successfully run a test rig rotor supported by the passive system to 50,000 rpm.

PM RADIAL BEARINGS

Our work in the application of PM bearings to flywheels began in the early 1990s [3]. These systems were composed of two identical passive PM bearings and an active magnetic thrust bearing. In one of our earlier designs, a PM bearing consisted of several concentric rings of identical magnetic structure for rotor and stator. The polarization directions of the PM rings were alternatively stacked up to trap the magnetic flux in the air gap and achieve a stiff passive bearing. There is a speed limitation to this approach, since each larger diameter ring is exposed to higher centrifugal loads. Nonetheless, we were able to make radially stacked bearings for design speeds up to 30,000 rpm.

For an ongoing NASA initiative (NAS3-02128) to develop a PM-based suspension system for a 60,000-rpm, 16-kg flywheel, an axial stack-up configuration appeared more feasible, and we have designed, fabricated, and tested such a bearing. On the rotor, there are identical, axially polarized PM rings. The rings are clamped together with identical poles facing each other. A similar magnetic structure exists on the stator, except that the ring diameter is larger. Thin copper sheets are imbedded in the bearing stator to create eddy current damping. Approximately 1% of critical damping ratio for resonance up to 2,000 Hz has been achieved based on experimental ringing-decay data.

Figure 1 shows several components of this PM radial bearing design, which consists of 10 PM rings, a rotor ring ID of 38.5 mm, a stator ring ID of 46.0 mm, a radial magnetic gap of 0.76 mm, a PM ring cross section of 3 x 3 mm, a PM remnant flux density of 1.0 T, and a measured radial stiffness of ≈ 263 N/mm (1,500 lb/in.).

Since the PM thickness is relatively much smaller than the average radius, R, at the gap, a 2-D finite-element static magnetic analysis was performed to predict bearing stiffness. Results of this analysis

indicated that repulsive force changes by 0.366 N for a gap change of 0.1 mm between the rotor and stator cross sections. This implies a linear stiffness K_1 = 0.366/0.1 = 3.66 N/mm per mm of depth into the paper. It is readily proved that the bearing radial stiffness is:

$$K_r \approx \pi R K_1 = \pi\,(22.62)(3.66) = 262\ \text{N/mm}$$

Note that the bearing has a negative axial stiffness (K_a) equal to –2 K_r or –524 N/mm and a negative angular stiffness of $K_\theta = K_r\,(L^2/12 - R^2)$ = -1.14 x 10^5/radian for this bearing with L = 30 mm and R = 22.62 mm. The value of K_θ is difficult to verify but appreciated during rotor/bearing assembly.

The ID hoop stress of the rotor PM ring is about 172 x 10^6 Pa (25 ksi) at 66,000 rpm, much higher than the tensile strength of the neodymium-iron-boron magnet material used in this application. Therefore, a radial preloaded Inconel sleeve supports the rotor ring magnets. Note from the above parameters that the radial gap is 0.75 mm. If the sleeve is 0.5-mm thick, the rotor can move radially 0.25 mm, and the corresponding load capacity would be 65 N (=263 x 0.25). To increase the stiffness, one may increase the diameter and/or number of rings [4, 5].

Spin tests for the PM bearings were conducted to 66,000 rpm in a commercial spin pit with no degradation of mechanical integrity or stiffness.

ACTIVE RADIAL DAMPER

In the flywheel application, additional damping is needed since the eddy-current damping is low and may be inadequate for controlling transient vibrations, such as traversing a critical speed or dampening shock response. A separate radial passive damper of the eddy-current type has been used before and consists of a conducting disk with its outer edge rotating in a uniform axial magnetic field. However, unlike active magnetic bearings, where the damping can, within limits, be adjusted as needed to change damping characteristics, the damping in passive magnetic bearings or eddy dampers is limited in value and fixed by design.

To design an active damper for our test rotor with PM bearings, we performed a critical speed analysis of the dynamic system using DyRoBeS™ , a commercial rotor dynamics program from Concepts NREC (www.conceptseti.com.). The resulting critical speed map indicated that below 60,000 rpm there are only two rigid-body critical speeds at about 1900 rpm and 3800 rpm. As shown in Figure 2, the first bending critical is at 81,000 rpm. At the chosen location of the damper, there are plenty of vibration mode shape displacements, and therefore the damper will be effective in controlling the vibration. A damping coefficient of 0.875 N-sec/mm (5 lb-sec/in.) was chosen for the damper, and it results in a log decrement value of 0.9 at the first critical speed, or a Q-factor of about 4, which is satisfactory and acceptable.

To size the damper, assume that the orbit at traversing the first critical is no more than 0.05 mm 0-pk (0.002 in. 0-pk). Then, the maximum damper transient force is about 8 N (≈ 0.875 N-sec/mm x 0.05 mm x 200 radial/sec). To minimize the number of poles and thus eddy-current loss, we selected a one-sided homopolar electromagnetic device with PM bias (see Figure 3). The laminated (silicon steel) pole area is 8 x 8 mm. The laminated journal is 25 mm in diameter. The PM bias flux at the poles was measured to be 5.5 kGs. The damper has a force capacity of 24 N, which is three times larger than the predicted maximum load.

ACTIVE THRUST BEARING

The active thrust bearing of the test rotor works against the axial stiffness of the PM radial bearings, about –1050 N/mm, as well as the rotor weight of 16 kg. We selected a conventional thrust bearing design, which includes a rotating disk and two single-coiled stators for push-and-pull actuation. The key parameters of the thrust bearing are: a load capacity of 600 N, a disk OD of 88 m, a disk ID of 45 mm, a 0.5-mm air gap, 150 coil turns per stator, a coil resistance of 2 Ω, and a nominal inductance of 15 mH.

A unique velocity feedback scheme [6, 7] with zero-force-seeking ability can be used to control the thrust bearing to eliminate the steady state or dc control currents in the coils. The rotor axial velocity signal is obtained by differentiating the axial displacement measurement. Although this scheme is simple in terms of its electronics, it is difficult to tune the control parameters. In addition to a using conventional proportional-integral-derivative (PID) control scheme, we have also planned to achieve the zero-power state for the thrust bearing, using a sliding-mode control (SMC) algorithm [8, 9] with automatic reference shift.

The axial vertical dynamics of the test rotor can be represented by:

$$M\frac{d^2Y}{dt^2} + K_{pm}Y = -MG + F_t - F_b \qquad (1)$$

where:

M	=	rotor mass
Y	=	rotor axial (vertical) displacement
d^2Y/dt^2	=	second derivative of displacement Y with respect to time t
G	=	gravitational constant
K_{pm}	=	axial magnetic stiffness due to PM radial bearings (negative value)
F_t	=	magnetic control force of top stator
F_b	=	magnetic control force of bottom stator

Using current-source power amplifiers, the coil current becomes essentially the control variable. The maximum current is that required for lifting the rotor off a backup bearing. The SMC performs feedback control on the axial displacement measurement based on a switching function:

$$S = C(Y - \delta) + \frac{dY}{dt} \quad (2)$$

The control current is calculated as:

$$I = -K\left|Y - \delta\right|\frac{S}{|S|} \quad (3)$$

where:

C = positive weighing constant
K = positive current constant
δ = displacement shift = $C_i \int I\,dt$
C_i = positive integral constant

We only energize one coil at a time, i.e., top coil current = I; bottom coil current = 0, if I > 0; top coil current = 0; bottom coil current = I, if I < 0.

Changing the weighing constant, C, modifies the system damping, i.e., more damping with smaller C. Larger K means tighter control of error.

Using C = 200 and K = 3000, a lift-off transient simulation of the test rotor under sliding mode thrust control was performed. The results are presented in Figure 4. The calculated displacement plot shows that the rotor rapidly settles to a position of 0.15 mm above the thrust bearing equilibrium point. Note that (0.15 mm)(1050 N/mm) = 158 N = 16 kg = rotor weight.

The current plot shows small regulating currents on the top or bottom coil. The effect of the transient currents, such as the eddy current loss in solid cores will be evaluated in tests.

TEST ROTOR PERFORMANCE

Our bearing-damper system test rig, including a vertically oriented 16-kg rotor, is shown in Figure 5. The rotor is 525 mm long. From the photograph, one may appreciate the small size of the active damper as compared to the other components. At this time, the thrust bearing is levitated with a conventional PID control. Preliminary tests of the fully levitated rotor showed the first critical speed at 1900 rpm with a bouncing mode, and the second critical speed at 3900 rpm with a conical mode. The first bending is at 78,000 rpm. These critical speeds are very close to the analytically predicted values. It took 50 min for the rotor to coast down from 5000 rpm in air. The damper and bearings apparently have very low power loss. It was very clear that without activating the damper the rotor would not be stable above the second critical speed.

The test rig was installed in a containment chamber for high-speed spinning tests. We were able to run the rotor up to 51,000 rpm. Some test results are presented as follows.

Figure 6 presents a typical frequency spectrum coastdown plot using a "peak-hold" mode in the frequency analyzer. The high-speed rotor displacement (mostly due to probe runout) is very flat, because the rotor runs at the mass center with soft PM bearings.

Figures 7 and 8 show frequency spectra at rotor speeds of 20, 30, 40 and 51 krpm. The subsynchronous shaft vibration at the first critical frequency apparently grew with the speed. The excitation appears aerodynamic in nature. In this regard, the PM bearings may have functioned as unloaded plain cylindrical air bearings and generated destabilizing cross-coupling stiffness, which is proportional to speed [10]. One would expect the excitation does not exist in a vacuum chamber as for the most flywheel applications. There are two possible reasons for the damper to be ineffective at high speeds: 1) eddy current effect saturates the core, and 2) there is a low frequency conical mode with a pivot close to the damper. Note that a subtle difference between this test rotor and a real flywheel is the low polar moment of inertia of the test rotor. It is difficult for the conical mode to exist due to a large gyroscopic inertia effect.

SUMMARY AND CONCLUSIONS

Several conclusions can be drawn from the work performed. First, an active radial damper is needed to supplement damping for traversing critical speeds and suppressing subsynchronous whirls. Second, a sliding mode control method is feasible as a means of control for the thrust magnetic bearing in the flywheel suspension system. Third, a passive magnet bearing system is well suited as a component in a magnetic-bearing-based suspension system for energy storage flywheels.

ACKNOWLEDGMENT

This work has been supported by NASA under Phase II SBIR contract NAS3-02128. The authors thank Foster-Miller management for permission to publish this paper.

REFERENCES

1. Chen H. M., W. Smith, and J. Walton. "A High Efficiency Magnetic Bearing for a Rotary Blood Pump." ASAIO 44th Annual Conference, New York, NY, October 1998.
2. Chen, H. M. et al. "Development of Magnetically Levitated Blood Pumps." 6th Int'l Symp. on Mag. Susp. Tech., Turin, Italy, October 7-11, 2001, pp. 30-36.

3. Tecza, J., N. Vitale, and H. M. Chen. "Development of Motor/Generator Technology for Flywheel Energy Storage Applications." MTI 95TR16, January 1995.
4. Yonnet, J. "Permanent Magnet Bearings and Couplings." IEEE Transactions on Magnetics, Vol. Mag-17, No.1, January 1981.
5. Yonnet, J., et al. "Stacked Structures of Passive Magnetic Bearings." J. Appl. Phys. 70(10), 15 November 1991.
6. "Velocity-Controlled Magnetic Bearings." U.S. Patent No. 5,666,014, September 9, 1997.
7. Chen, H. M. "Design and Analysis of a Sensorless Magnetic Damper." 95GT180, ASME Turbo Expo, Houston, TX, June 1995.
8. Utkin, V., J. Guldner, and J. Shi. *Sliding Mode Control in Electromechanical Systems*, Taylor & Francis, 1999.
9. Allaire, P.E. and A. Sinha. "Robust Sliding Mode Control of a Planar Rigid Rotor System on Magnetic Bearings." 6th Int'l Symp. on Mag. Brg, Cambridge, MA, August 5-7, 1998.
10. Lee, C. W. *Vibration Analysis of Rotors*, Chapter 3, Kluwer Academic Publishers, 1993.

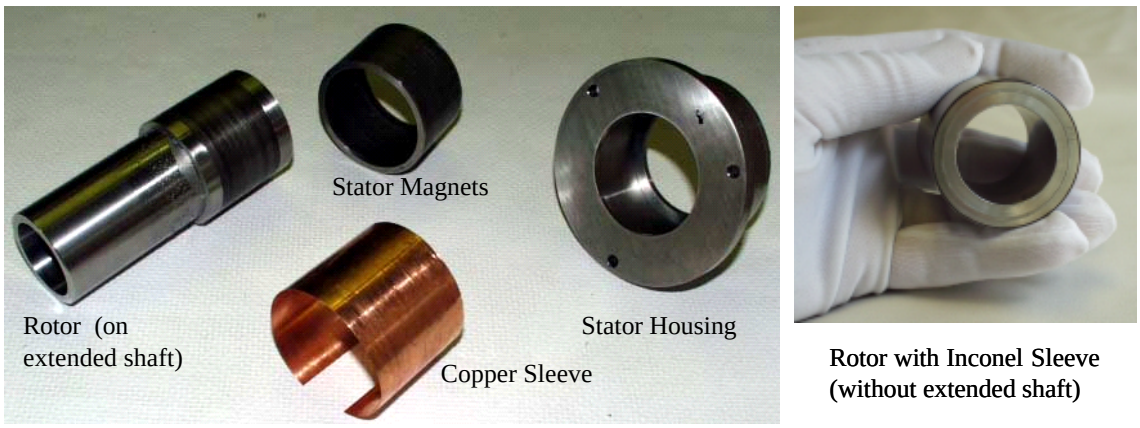

Figure 1. PM Radial Bearing Components

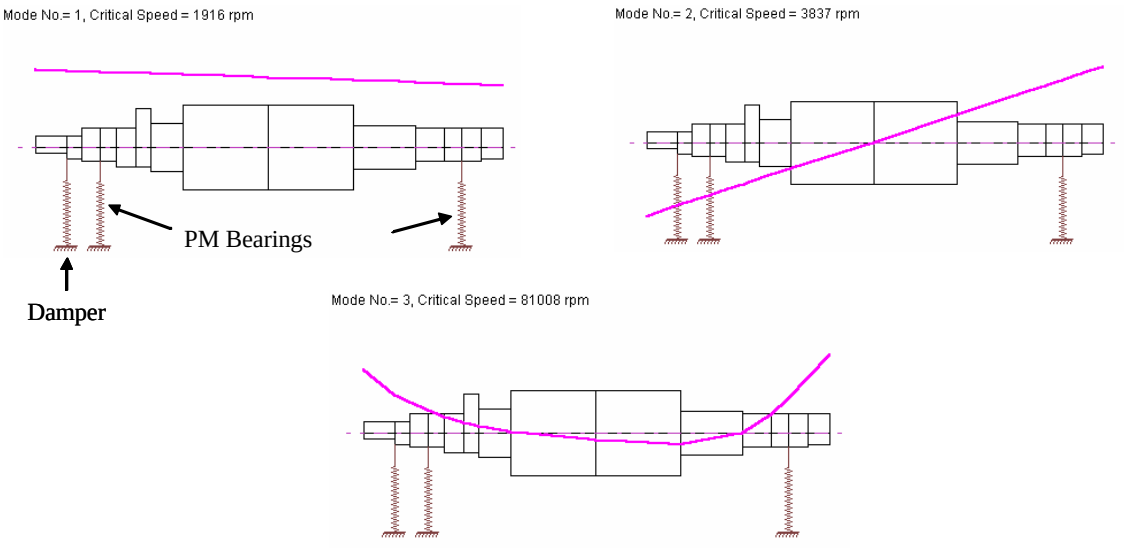

Figure 2. Rotor Critical Speed Modes

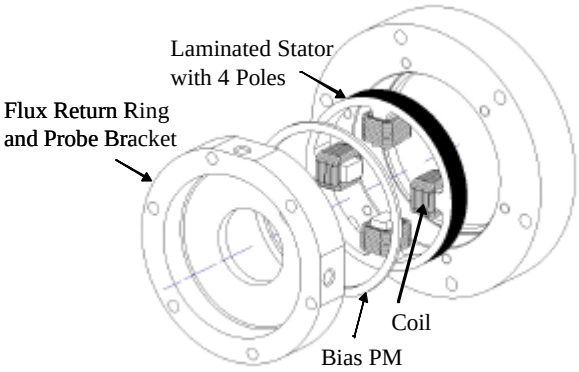

Figure 3. Active Damper Design

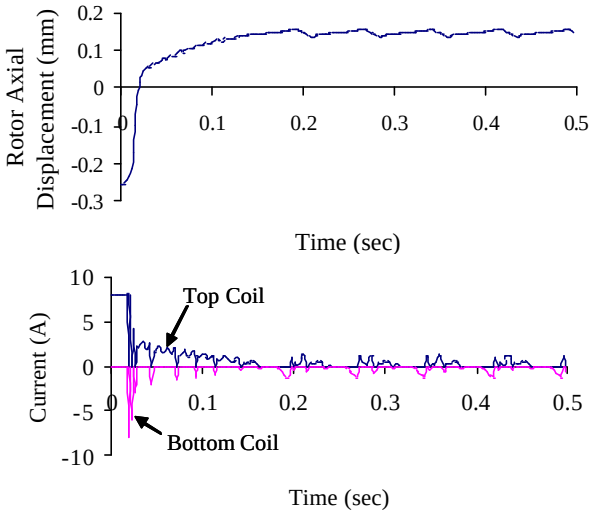

Figure 4. Thrust Bearing SMC Simulation

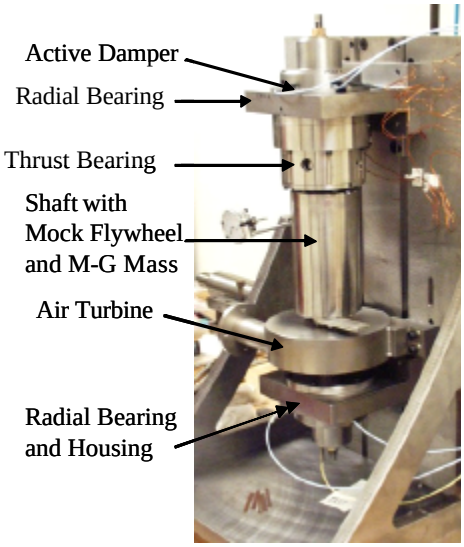

Figure 5. Test Rotor Hardware

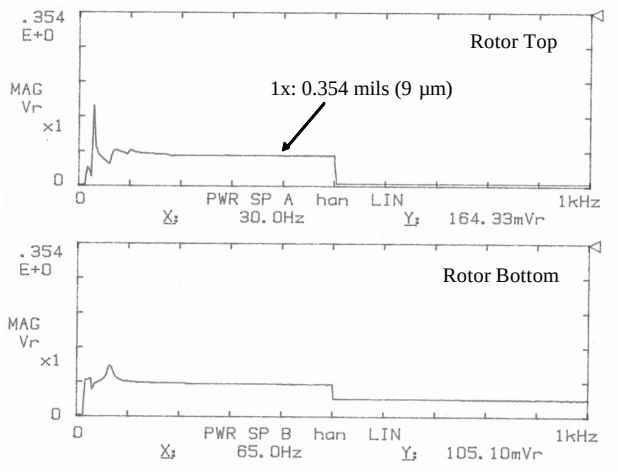

Figure 6. Coastdown from 30,000 rpm

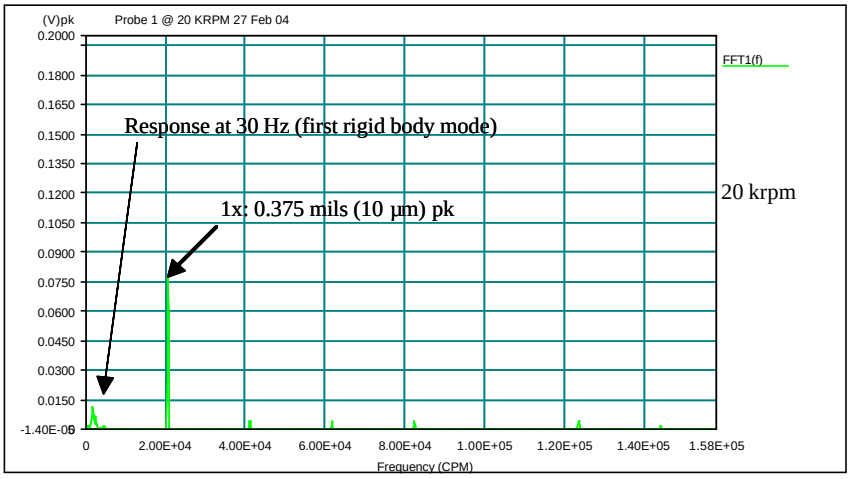

Figure 7. Displacement Frequency Spectra at 20 krpm

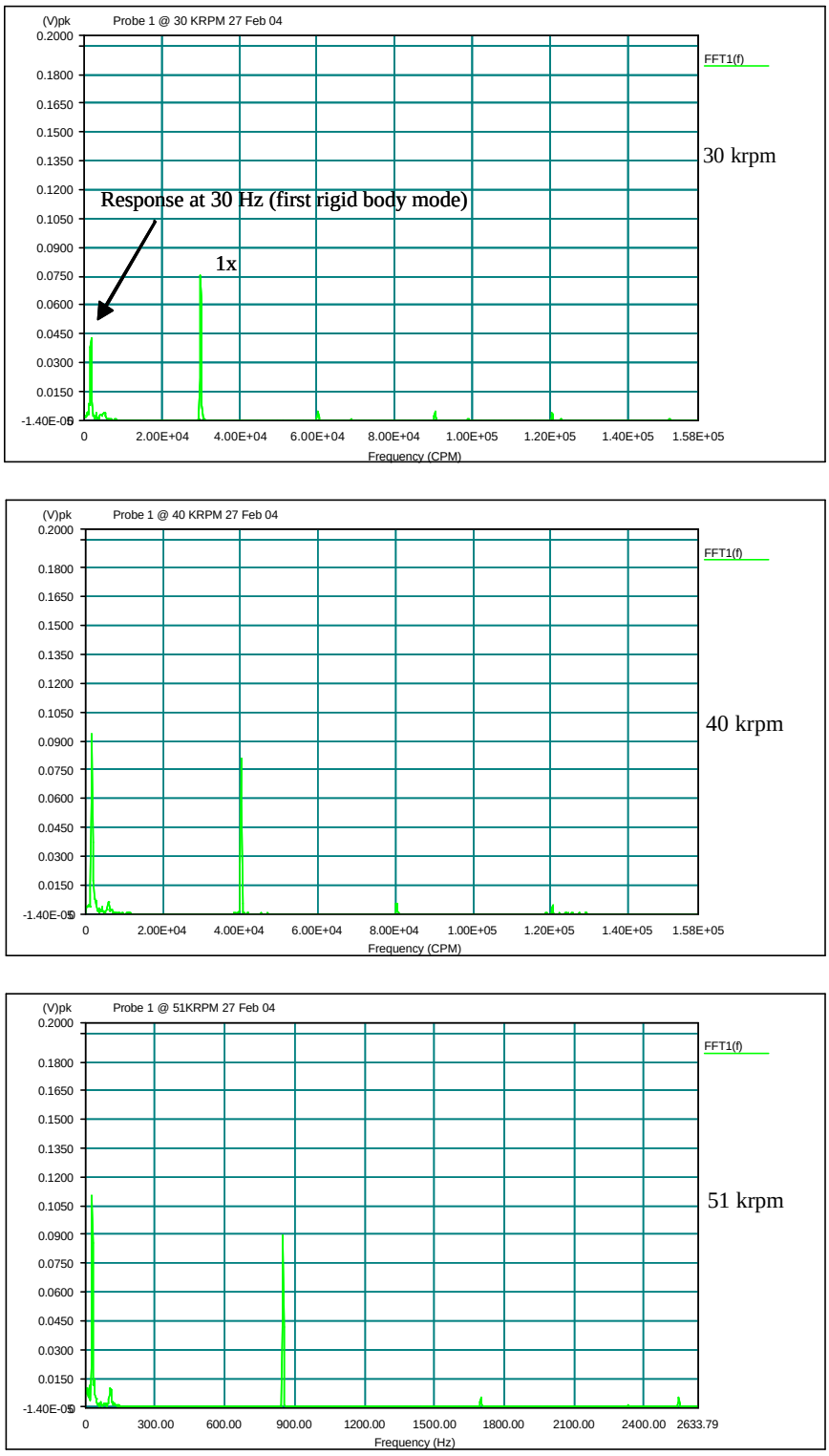

Figure 8. Displacement Frequency Spectra at 30, 40, and 51 krpm